Overlapping sequence of doubly excited series in the vuv spectrum of argon

M. Aslam Baig and Sultan Ahmad
Atomic and Molecular Physics Laboratory, Department of Physics, Quaid-i-Azam University, Islamabad, Pakistan

J. P. Connerade
Blackett Laboratory, Imperial College, London SW7 2BZ, United Kingdom

Wolfgang Dussa and Josef Hormes
Physikalisches Institut der Universität Bonn, 5300 Bonn 1, Nussallee 12, Federal Republic of Germany
(Received 26 August 1991)

Observations of overlapping sequences of doubly excited resonances in the absorption spectrum of argon are reported at improved resolution, exhibiting more detail than earlier studies. Their appearance is compared with the doubly excited manifolds recently reported in the spectrum of He by Domke *et al.* [Phys. Rev. Lett. **66**, 1306 (1991)] and by Zubek *et al.* [J. Phys. B **24**, L342 (1991)]. The salient differences are pointed out and their origin is explained. The simplest case of overlapping channels has been accounted for by Lane's theory [J. Phys. B **17**, 2213 (1984)] for one broad intruder in a Rydberg series of autoionizing resonances. Numerous interesting examples of the q-reversal effect are uncovered.

PACS number(s): 32.30.Jc, 32.80.Dz, 32.80.Fb, 32.70.Jz

Double excitations appear in the photoabsorption spectra of atoms as families of series, which become more numerous and more crowded as the double-ionization threshold is approached. In He, the double-ionization threshold stands well above all single excitations, so that, although the doubly excited spectrum contains much detailed structure, its overall appearance is quite regular, as demonstrated by recent data (Domke *et al.* [1] and Zubek *et al.* [2]).

As one moves to heavier rare gases, there are many reasons for which this overall regularity can be lost. First, the manifold of doubly excited channels moves down closer to the single excitations, which themselves become more numerous owing to excitations from inner shells. Thus, single and double excitations are no longer well separated in energy. This has two consequences: first, there is usually an enhancement of double-excitation spectra at the expense of the single excitations, and second, both classes of spectra lose some of their regularity.

Another effect to be considered is the appearance of multiplet structure in the parent ion. Indeed, helium is the only rare gas for which the parent ion is hydrogenic, so that, with increasing excitation energy, doubly excited manifolds converge on successive, initially well-separated thresholds of different principal quantum number N of the parent ion. In all other rare gases, multiplet structure due to the open p^4 subshell will be present even for the lowest excitations. Thus, in all other rare gases, overlapping resonances occur even amongst the lowest double-excitation channels, which are relatively unperturbed in He.

A further complication is that, as the onset of orbital contraction in the first long periods is approached, the doubly excited spectra involve both *ns* and *nd* electrons, whose behavior in homologous sequences exhibits the systematic trends characteristic of orbital collapse (Connerade [3]). A case of particular interest in this respect is Ar, because it lies just before the first transition sequence.

A combination of high experimental resolution and broad coverage of a wide spectral range, such as can only be achieved with synchrotron radiation, is required in order to study doubly excited manifolds of Rydberg series. In the present paper, we report observations over the full energy range of the parent-ion terms $3s^2 3p^4(^1S, ^3P$, and $^1D)4s$, $4p$, and $3d$. Interestingly, not all possible manifolds are observed: the spectrum is dominated by a small number of channels.

Experiments were performed at the 2.5-GeV electron synchrotron of the Physikalisches Institut in Bonn, using a high-resolution 3-m normal-incidence spectrograph equipped with a 5000 line/mm holographic grating. Details of the apparatus and techniques have previously been published (Baig *et al.* [4–6]). Wavelength calibration was obtained by comparison with the sharp lines of the same spectrum as previously recorded by Baig and Ohno [7] and Madden *et al.* [8]. The absolute accuracy of the observed spectral lines is ± 0.008 Å achieved by using the third-order Chebychev-polynomial fit. The spectra recorded on the photographic plates were digitized with a computer-controlled microdensitometer. The transmission of the blackened photographic plate was measured in steps of 5 μm using a slit width of 10 μm at the photomultiplier. One photographic plate of 20-cm length covers a spectral range of roughly 120 Å. The digitized spectrum therefore consists of about 40 000 data points. As the response curve of the photographic emulsion is nonlinear, the plotted profile is not proportional to the absorption cross section. Relative intensities are, however, correct when lines on the same exposure are compared which lie on the linear part of the response curve.

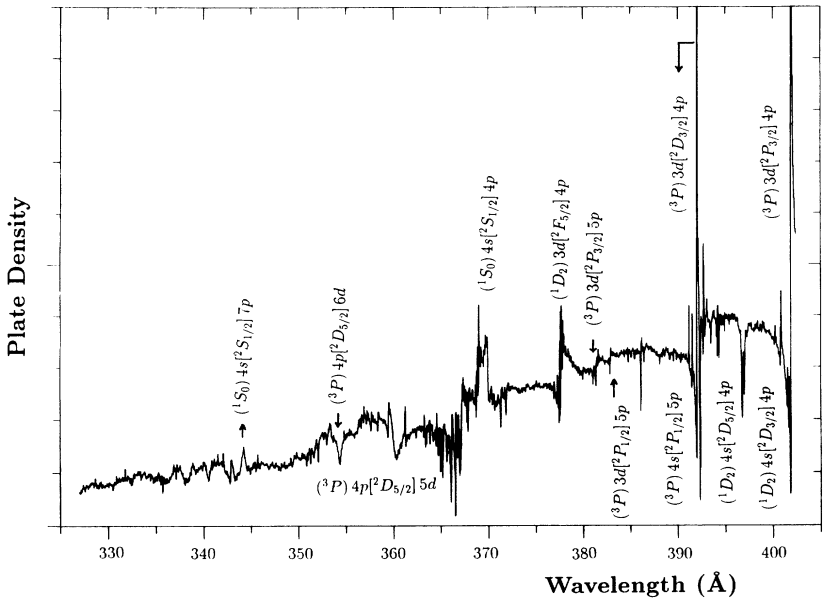

FIG. 1. The absorption spectrum of Ar I, showing the complete spectrum covering the spectral region between 320 and 400 Å. The identifications for the resonance between 370 and 400 Å are taken from Madden *et al.* [8].

The present spectrum provides much improved detail as compared with the earlier work of Madden *et al.* [8]. The experimental spectra we have obtained are shown in Figs. 1–3. From our observations and the series limits listed in the tables of Moore [9], fairly constant quantum defects for the different channels have been extracted, which allow quite reliable groupings into Rydberg series to be achieved, once account is also taken of the pronounced intensity perturbations which the broadest lowest members of each channel produce amongst the higher members of the next channel down in energy, a situation strongly reminiscent of the interactions found by Domke *et al.* [1] between the $N=5$ and 6 doubly excited channels of He.

The $3s$ inner-shell excitation spectra

$$3s^2 3p^6(^1S_0) \Longrightarrow 3s(^6S_{1/2})3p^6 np\ ^1P_1\ ,$$

exhibiting window-type autoionizing resonances, were re-

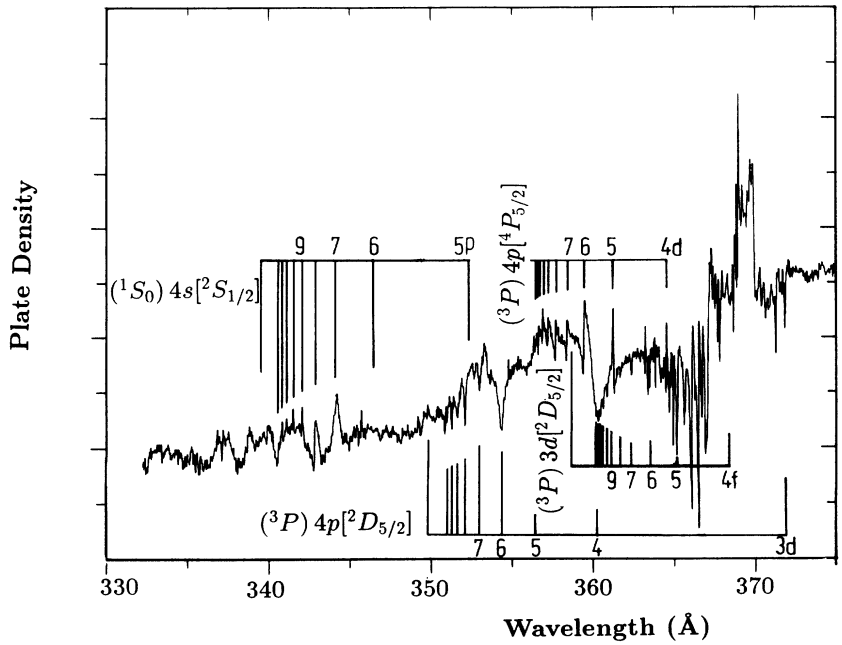

FIG. 2. The absorption spectrum of Ar I, showing the double-excited Rydberg series terminating to four high-lying limits (see text for details). The intensity variations are due to the low-lying members of the series belonging to the other channels, particularly around 367, 360, and 354 Å.

TABLE I. Broad resonances series; the leading member was picked up by looking at the interesting variation around 366 Å. $3s^23p^6\,{}^1S_0 \rightarrow 3s^23p^4({}^1S_0)4s\,({}^2S_{1/2})np\,{}^1P_1$.

nl	Wavelength (Å)	Wave number (cm^{-1})	n^*
$4p$	366.2[a]	273 075	2.324
$5p$	352.2[a]	283 930	3.351
$6p$	346.428[b]	288 660.3	4.365
$7p$	344.202	290 527.1	5.310
$8p$	342.858	291 666.0	6.314
$9p$	342.034	292 368.6	7.316
$10p$	341.496	292 829.2	8.309
$11p$	341.098	293 170.9	9.378
$12p$	340.842	293 391.1	10.334
Limit		294 418.56	

[a]Overlapping.
[b]Very weak.

ported by Baig and Ohno [7]. In the present work, the following two-electron transitions are considered:

$$3s^23p^6({}^1S_0) \Longrightarrow 3s^23p^4({}^3P,{}^1D_2,{}^1S_0)3dnp,nf$$
$$\Longrightarrow 3s^23p^4({}^3P,{}^1D_2,{}^1S_0)4snp$$
$$\Longrightarrow 3s^23p^4({}^3P,{}^1D_2,{}^1S_0)4pns,nd\ .$$

A remarkable phenomenon is the following: although, within the energy range presently studied, there are 24 terms of the $3s^23p^44s$, $4p$, and $3d$ complex, which can in principle produce a vast number of accessible series limits of different J values; Rydberg sequences to only nine distinguishable thresholds have been observed. Again, one can perhaps draw a comparison with He, for which unexpected simplicity of structure is found in the doubly excited spectrum (Fano [10]).

More specifically, we observe one series attaching to the term $3s^23p^4({}^1S_0)4s\,({}^2S_{1/2})$, which must be an np series with $J=1$ and is the only possible combination with the ground state for this term of the parent ion. The data for this series are tabulated in Table I. For the $3s^23p^4({}^1D_2)4s\,({}^2D)$ term, we only observe one nf series to

TABLE II. Window-type autoionizing resonance series, $3s^23p^6\,{}^1S_0 \rightarrow 3s^23p^4({}^1D)4s\,({}^2D_{3/2})nf\,{}^1P_1$.

nl	Wavelength (Å)	Wave number (cm^{-1})	n^*
$4f$	371.843	268 930.7	4.017
$5f$	368.705	271 219.6	4.932
$6f$	366.746	272 668.3	5.986
$7f$	365.667	273 472.9	6.971
$8f$	364.960[a]	274 002.7	7.968
$9f$	364.483	274 361.2	8.951
$10f$	364.133	274 625.0	9.961
$11f$	363.858	274 832.5	11.052
Limit		275 730.88	

[a]Overlapping.

TABLE III. This series shows anomalous intensity behavior at high n values ($11 \le n \le 22$) which is due to mixing with the autoionizing resonance around 377 Å. Madden *et al.* [8] have assigned this resonance as $({}^1D_2)3d\,({}^2F_{5/2})4p$. $3s^23p^6\,{}^1S_0 \rightarrow 3s^23p^4({}^3P_0)4s\,({}^2P_{3/2})np\,({}^1P_1)$.

nl	Wavelength (Å)	Wave number (cm^{-1})	n^*
$5p$	392.726	254 630.5	3.199
$6p$	386.375	258 815.9	4.097
$7p$	382.872	261 183.9	5.130
$8p$	381.068	262 420.4	6.116
$9p$	380.034	263 134.4	7.031
$10p$	379.275	263 661.0	8.050
$11p$	378.786	264 001.3	9.005
$12p$	378.410	264 263.6	10.030
$13p$	378.137	264 454.5	11.042
$14p$	377.898	264 621.7	12.237
$15p$	377.727	264 741.5	13.380
$16p$	377.622	264 815.1	14.264
$17p$	377.550	264 865.6	14.983
$18p$	377.444	264 940.0	16.272
$19p$	377.384	264 982.1	17.168
$20p$	377.328	265 021.4	18.153
$21p$	377.274	265 059.4	19.286
$22p$	377.241	265 082.5	20.090
$23p$	377.206	265 107.1	21.066
$24p$	377.172	265 131.0	22.164
Limit		265 354.41	

the $({}^2D_{3/2})$ limit, although an np electron attaching to either the ${}^2D_{3/2}$ or ${}^2D_{5/2}$ limit could result in accessible levels. The tentative level assignments are based on the observed quantum-defect values listed in Table II.

Turning now to the $3s^23p^4({}^3P)$-based limits, we again find one np series to the limit involving a $4s$ electron, namely $3s^23p^4({}^3P_0)4s\,({}^2P_{3/2})$, which is listed in Table III. For the limits involving a $4p$ electron, two series are found, one nd series to $3s^23p^4({}^3P)4p\,({}^2D_{5/2})$ (see Table

TABLE IV. Window-type autoionizing resonances series; assignment as $ns[\frac{5}{2}]$ series is discarded as is does not combine with the ground-state ${}^1S_0$. The $4d\,{}^1P_1$ member lies at the threshold of $3s^23p^4({}^3P_1)3d\,({}^2D_{5/2})nf$ series. $3s^23p^6\,{}^1S_0 \rightarrow 3s^23p^4({}^3P)4p\,({}^2D_{5/2})nd\,{}^1P_1$.

nl	Wavelength (Å)	Wave number (cm^{-1})	n^*
$3d$	371.843	268 930.7	2.547
$4d$	360.86[a]	277 114.3	3.546
$5d$	356.381	280 598.6	4.575
$6d$	354.339	282 215.6	5.502
$7d$	352.994	283 291.0	6.560
$8d$	352.211	283 920.7	7.559
$9d$	351.674	284 354.3	8.591
$10d$	351.315	284 644.8	9.578
$11d$	351.055	284 855.7	10.553
$12d$	350.859	285 014.8	11.524
Limit		285 841.10	

[a]Broad.

TABLE V. Asymmetric autoionizing resonance series, $3s^23p^6\,{}^1S_0 \rightarrow 3s^23p^4({}^3P)4p\,({}^4P_{5/2})nd\,{}^1P_1$.

nl	Wavelength (Å)	Wave number (cm^{-1})	n^*
$3d$	372.07	268 768.1	2.960
$4d$	364.562	274 301.8	3.963
$5d$	361.213	276 845.0	4.969
$6d$	359.475	278 183.5	5.944
$7d$	358.389	279 026.4	6.963
$8d$	357.705	279 560.0	7.965
$9d$	357.237	279 926.2	8.971
$10d$	356.905	280 186.6	9.973
$11d$	356.656	280 382.2	10.996
Limit		281 289.79	

IV), one nd series to $3s^23p^4({}^3P)4p\,({}^4P_{5/2})$, listed in Table V and none to any $J_c = \frac{1}{2}$ or $\frac{3}{2}$ limits. We attribute the series to the excitation of an nd electron because the lowest effective quantum number is nearly equal to 3.

For the limits involving a $3d$ electron, we find series to four limits: $3s^23p^4({}^3P)3d\{{}^2D_{5/2}, {}^2F_{5/2}, {}^2P_{3/2}$, and ${}^2P_{1/2}\}$; again, there is one series to each limit. Wavelengths of all these observed series are listed in Tables VI–IX, respectively. An interesting observation is that for a Rydberg series attaching to high angular momentum of the core (${}^2D_{5/2}$ or ${}^2F_{5/2}$), the effective quantum numbers are nearly hydrogenic (see Tables VI and VII), whereas for lower angular momentum of the core (${}^2P_{3/2}$ or ${}^2P_{1/2}$), the effective quantum numbers are as one would expect for a penetrating np series (see Tables VIII and IX).

It is interesting that we observe series to all possible terms involving a $4s$ electron, which indicates that the excitation processes from the $3s^23p^6\,{}^1S_0$ ground state favor doubly excited configurations involving $4s$ over $4p$ or $3d$. In short, we are finding far fewer series than the selection rules allow, but it is not obvious what new rules should be used to predict which are the strong double excitations.

TABLE VI. Weak window-type autoionizing resonance series, $3s^23p^6\,{}^1S_0 \rightarrow 3s^23p^4({}^3P)3d\,({}^2D_{5/2})nf\,{}^1P_1$.

nl	Wavelength (Å)	Wave number (cm^{-1})	n^*
$4f$	368.279	271 533.3	4.058
$5f$	365.179	273 838.3	5.017
$6f$	363.396	275 181.9	6.032
$7f$	362.327	275 993.8	7.056
$8f$	361.637	276 520.4	8.087
$9f$	361.213	276 845.0	9.005
$10f$	360.862	277 114.3	10.062
$11f$	360.603	277 313.3	11.136
$12f$	360.430	277 446.4	12.082
$13f$	360.291	277 553.5	13.047
Limit		278 198.08	

TABLE VII. Window-type autoionizing resonance series, $3s^23p^6\,{}^1S_0 \rightarrow 3s^23p^4({}^3P)3d\,({}^2F_{5/2})nf\,{}^1P_1$.

nl	Wavelength (Å)	Wave number (cm^{-1})	n^*
$4f$	371.279	269 339.2	3.973
$5f$	367.975	271 757.6	4.920
$6f$	366.082	273 162.9	5.924
$7f$	364.960[a]	274 002.7	6.926
$8f$	364.224	274 556.3	7.956
$9f$	363.738	274 923.2	8.960
$10f$	363.396	275 181.9	9.951
$11f$	363.146	275 371.4	10.929
Limit		276 290.08	

[a]Overlapping.

TABLE VIII. Series $3s^23p^6\,{}^1S_0 \rightarrow 3s^23p^4({}^3P)3d\,({}^2P_{3/2})np\,{}^1P_1$.

nl	Wavelength (Å)	Wave number (cm^{-1})	n^*
$4p$	396.7	252 080	2.302
$5p$	381.358	262 220.8	3.224
$6p$	374.723[a]	266 863.8	4.307
$7p$	371.843	268 930.7	5.339
$8p$	370.319	270 037.5	6.326
$9p$	369.313	270 773.0	7.395
$10p$	368.705	271 219.6	8.387
$11p$	368.279	271 533.3	9.383
$12p$	367.975	271 757.6	10.361
$13p$	367.742	271 929.8	11.362
$14p$	367.570	272 057.0	12.322
$15p$	367.427	272 162.9	13.338
$16p$	367.310	272 249.6	14.387
$17p$	367.224	272 313.4	15.339
Limit		272 779.74	

[a]Very weak.

TABLE IX. Series $3s^23p^6\,{}^1S_0 \rightarrow 3s^23p^4({}^3P)3d\,({}^2P_{1/2})np\,{}^1P_1$.

nl	Wavelength (Å)	Wave number (cm^{-1})	n^*
$4p$	393.065	254 410.9	2.511
$5p$	380.001[a]	263 157.2	3.559
$6p$	375.373[a]	266 401.7	4.500
$7p$	372.866	268 192.9	5.500
$8p$	371.378	269 267.5	6.556
$9p$	370.574	269 851.6	7.465
$10p$	369.934	270 318.5	8.547
$11p$	369.520	270 621.4	9.565
$12p$	369.223	270 839.0	10.572
$13p$	368.994	271 007.1	11.613
$14p$	368.848	271 114.4	12.464
$15p$	368.705	271 219.6	13.510
Limit		271 820.80	

[a]Very weak.

A remarkable effect in the spectrum is the approximate alternation of the asymmetry parameters q between successive series as the highest observed parent-ion state $3s^2 3p^4(^1S_0)4s$ is approached from below. Each series can be characterized by a given average q value. Thus, for example, the highest energy $3s^2 3p^4(^1S_0)4s(^2S_{1/2})np$ series possesses a large effective q value, corresponding to nearly asymmetric absorption peaks. The next down in energy, $3s^2 3p^4(^3p)4p(^2D_{5/2})nd$ series, possesses a small mean value of q, characteristic of nearly symmetric windows. The next one down, $3s^2 3p^4(^3P)4p(^4P_{5/2})nd$ series, has negative q, with a pronounced q reversal (Connerade [11], Baig and Connerade [12] and Connerade *et al.* [13]), giving positive q for the lower member. This q reversal is especially interesting as an example of a case in which the perturber is actually a window resonance, for which q is nearly zero. Within the perturbed series converging on $3s^2 3p^4(^3P)4p(^4P_{5/2})$, there is the further remarkable effect that the higher members are broad while the lower members are sharp. One could seek to explain this as resulting from an increase in the autoionization rate due to the presence of a new continuum above the $3s^2 3p^4(^3P)3d(^2D_{5/2})$ threshold, but it seems more likely, in view of the change in symmetry just referred to and the absence of similar broadenings as the other thresholds in the spectrum are crossed, that the effect is in fact a fluctuation in width of the type discussed by Connerade and Lane [14].

Indeed, the approach of Lane [15] is a useful framework within which to describe the kind of interactions between autoionizing resonances which are observed in the present spectrum. Thus, the lowest-energy series (where the interactions are simplest) has been fitted to the relation (Lane [15])

$$\sigma=\sigma_0(1-\rho_n^2)+\sigma_0\rho_n^2\frac{(q_n+\varepsilon_n)^2}{1+\varepsilon_n^2}\ ,$$

where

$$\varepsilon_n=\frac{[E-E_n-F_n(E)]}{\frac{1}{2}\Gamma_n}\ ,$$

$$q_n=\frac{(1+\varepsilon_{nB}^2)Z-(s+q_B^{-1})+\varepsilon_{nB}(1-sq_B^{-1})}{(1+\varepsilon_{nB}^2)u+\varepsilon_{nB}(s+q_B^{-1})+(1-sq_B^{-1})}\ ,$$

$$\rho_n=\frac{(1+\varepsilon_{nB}^2)u+\varepsilon_{nB}(s+q_B^{-1})+(1-sq_B^{-1})}{\{(\Gamma_n/\Gamma_n^0)(1+\varepsilon_{nB}^2)[W^2(1+\varepsilon_{nB}^2)+(1+2\varepsilon_{nB}q_B^{-1}-q_B^{-2})]\}^{1/2}}\ ,$$

$$F_n=\Gamma_n^0\tfrac{1}{2}t^2(1+\varepsilon_{nB}^2)^{-1}[(1-s^2)\varepsilon_{nB}-2s]\ .$$

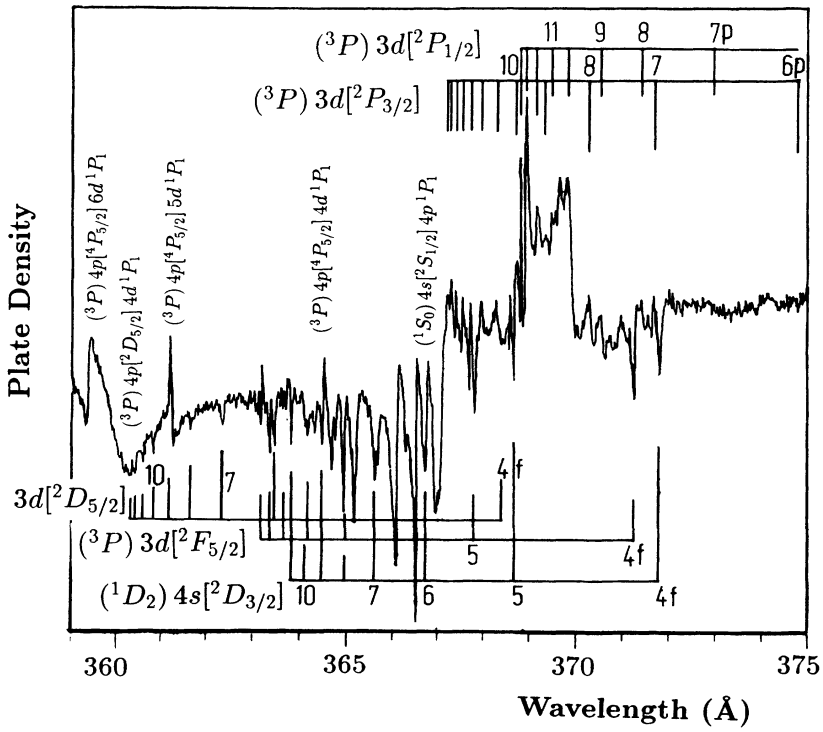

FIG. 3. The absorption spectrum of argon showing an enlarged portion of the spectrum between 360 and 375 Å. The Rydberg series converging to five limits are marked.

TABLE X. Values of parameters as obtained from our fit. Index B indicates values for the broad underlying state. The width of the Rydberg-series members is calculated after $\Gamma_n^0=\Gamma^0/(n^*)^3$.

Parameter	Value
$E_{\lim}$	265 325.26 cm^{-1}
μ	1.898
Γ^0	76 014.12 cm^{-1}
u	−17.52
s	1.262×10^{-8}
t	9.229×10^{-5}
W	21.52
z	2.00
σ_0	44 976.764
E_B	264 807 cm^{-1}
Γ_B	2372 cm^{-1}
q_B	−0.047

This is valid in the presence of several continua for narrow resonances and one broad state, by summing over a finite sequence of resonances and assuming their unperturbed oscillator strengths decrease as $1/n^3$. The result of the fit is shown in Fig. 4 whereas the parameters obtained are listed in Table X.

It is interesting to compare our conclusions with the photoelectron-satellite studies by Wills *et al.* [16], which show pronounced resonance structure in the relative intensities of the satellites which arise by decay into the parent ionic states. Unfortunately, the band pass of the primary photon excitation in the photoelectron study is only 75 meV. Thus, the series in their spectra can only be followed up to the fourth members whereas, in the most favorable cases, we follow series up to the 19th member. For this reason, most of the complex interactions we describe are not visible in the photoelectron data.

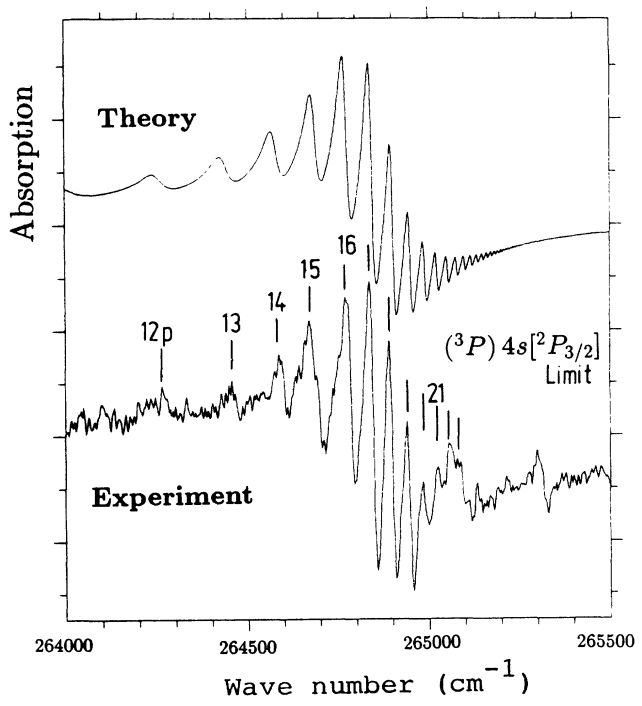

FIG. 4. Densitometer trace of the series converging to the $3s^23p^4(^3P)4s(^2P_{3/2})$ limit. The intensity variation between $n=11,\ldots,22$ is due to the $(^1D_2)3d(^2F_{5/2})4p$ perturber. The upper part of the figure is the fitted profile for an autoionizing Rydberg series interacting with a broad feature using Lane's formalism. The parameters are given in the text.

We thank Professor W. R. S. Garton of Imperial College London and Professor G. Noeldeke of the Physikalisches Institut der Universität Bonn for their interest and support. Financial support from the BMFT (F.R.G.) special funds for synchrotron radiation and the SERC (U.K.) as well as from the NSRDB (Pakistan) is gratefully acknowledged. One of us (M.A.B.) is grateful to the Alexander von Humboldt Stiftung (F.R.G.) for support during visits to the PI Bonn, where the present experiments were performed.

[1] M. Domke, C. Xue, A. Puschmann, T. Mandel, E. Hudson, D. A. Shirley, G. Kaindl, C. H. Greene, H. R. Sadeghpour, and H. Petersen, Phys. Rev. Lett. **66**, 1306 (1991).
[2] M. Zubek, C. Dawber, R. I. Hall, L. A. Avaldi, K. Ellis, and G. C. King, J. Phys. B **24**, L342 (1991).
[3] J. P. Connerade, J. Phys. B **24**, 605 (1991).
[4] M. A. Baig, J. P. Connerade, C. Mayhew, G. Noeldeke, and M. Seaton, J. Phys. B **17**, L383 (1984).
[5] M. A. Baig and J. P. Connerade, J. Phys. B **17**, 1785 (1984).
[6] M. A. Baig, A. Rashid, I. Ahmad, M. Rafi, J. P. Connerade, and J. Hormes, J. Phys. B **23**, 3489 (1990).
[7] M. A. Baig and M. Ohno, Z. Phys. D **3**, 369 (1986).
[8] R. P. Madden, D. L. Ederer, and J. Codling, Phys. Rev. A **177**, 136 (1969).
[9] C. E. Moore, *Atomic Energy Levels*, Natl. Bur. Stand. Ref. Data Ser., Natl. Bur. Stand. (U.S.) Circ. No. 35 (U.S. GPO, Washington, DC, 1971), Vol. I.
[10] U. Fano, Rep. Proc. Phys. **46**, 97 (1983).
[11] J. P. Connerade, Proc. R. Soc. London Ser. A **362**, 361 (1978).
[12] M. A. Baig and J. P. Connerade, J. Phys. B **18**, 3487 (1985).
[13] J. P. Connerade, A. M. Lane, and M. A. Baig, J. Phys. B **18**, 3507 (1985).
[14] J. P. Connerade and A. M. Lane, J. Phys. B **20**, 1757 (1987).
[15] A. M. Lane, J. Phys. B **17**, 2213 (1984).
[16] A. A. Wills, A. A. Cafolla, F. I. Currell, J. Corner, A. Svensson, and M. A. MacDonald, J. Phys. B **22**, 3217 (1989).